Rapid Communications

Domain wall melting in the spin-$\frac{1}{2}$ XXZ spin chain: Emergent Luttinger liquid with a fractal quasiparticle charge

Mario Collura,[1] Andrea De Luca,[2] Pasquale Calabrese,[1,3,4] and Jérôme Dubail[5]

[1]*SISSA, Via Bonomea 265, 34136 Trieste, Italy*

[2]*Laboratoire de Physique Théorique et Modélisation (CNRS UMR 8089), Université de Cergy-Pontoise, F-95302 Cergy-Pontoise, France*

[3]*INFN, Via Bonomea 265, 34136 Trieste, Italy*

[4]*International Centre for Theoretical Physics (ICTP), I-34151, Trieste, Italy*

[5]*Laboratoire de Physique et Chimie Théoriques, CNRS, UMR 7019, Universitè de Lorraine, 54506 Vandoeuvre-les-Nancy, France*

(Received 27 January 2020; revised 24 September 2020; accepted 2 November 2020; published 23 November 2020)

In spin chains with local unitary evolution preserving the magnetization S^z, the domain-wall state $|\ldots\uparrow\uparrow\uparrow\uparrow\uparrow\downarrow\downarrow\downarrow\downarrow\downarrow\ldots\rangle$ typically "melts." At large times, a nontrivial magnetization profile develops in an expanding region around the initial position of the domain wall. For nonintegrable dynamics, the melting is diffusive, with entropy production within a melted region of size $\sqrt{t}$. In contrast, when the evolution is integrable, ballistic transport dominates and results in a melted region growing linearly in time, with no extensive entropy production: The spin chain remains locally in states of zero entropy at any time. Here we show that, for the integrable spin-1/2 XXZ chain, low-energy quantum fluctuations in the melted region give rise to an emergent Luttinger liquid which, remarkably, differs from the equilibrium one. The striking feature of this emergent Luttinger liquid is its quasiparticle charge (or Luttinger parameter K), which acquires a fractal dependence on the XXZ chain anisotropy parameter Δ.

DOI: 10.1103/PhysRevB.102.180409

Introduction. The phenomenon of domain-wall (DW) melting in quantum magnetism is a simple example of quantum many-body dynamics. It has a long history in the context of quantum spin chains, dating back to early experimental work on $CoCl_2 \cdot 2H_2O$ chains [1], which provided the initial motivation for many subsequent theoretical developments. Those include studies of the dynamical stability of domain walls [2–5], exact calculations of magnetization profiles in free fermion chains [6–16], and approximate and numerical analyses both in integrable and nonintegrable spin chains [17–32].

On the analytical side, the 2016 discovery of a hydrodynamic approach to quantum integrable systems [33,34], now dubbed *generalized hydrodynamics* (GHD), has provided the ultimate analytical tool to analyze inhomogeneous dynamics of integrable systems [35–43], even in the classical context [44–46]. Its application to domain-wall melting in integrable spin chains has been particularly effective, providing the exact magnetization profile at large time for the XXZ chain [47] (see below).

Much effort has been spent to extend such a powerful method and include diffusive or superdiffusive effects [48–52], nonballistic phenomena [53], and integrability breaking [54–56] so as to codify correlations [57–62] and entanglement [63–66]. Indeed, due to its own coarse-grained nature, GHD in its original form cannot account for entanglement generation and quantum correlation spreading following the quantum unitary evolution. As a matter of fact, an uncorrelated initial state—e.g., a product state with zero entanglement—does develop entanglement when it evolves under a nontrivial unitary evolution. Recently, a low-energy description in terms of multicomponent Luttinger liquids (LL) [67–69] has been put forward [70]; such refined "quantum" adaptation of the GHD has been tested for integrable quantum gases [70]. Here we further develop this intuition and explore the nonequilibrium dynamics from a domain-wall (DW) state in the XXZ spin-1/2 chain, a genuinely interacting integrable model. Despite the simple structure of the initial state, the dynamics is highly nontrivial [47]; interestingly, the emerging local quasistationary state (LQSS) [33,71–73] admits a description in terms of two species of particles, each supporting a single Fermi point. In the spirit of the quantum GHD picture [70], we show that the quantum fluctuations in the LQSS can be exactly encoded in a LL, whose Luttinger parameter is nontrivial and differs from the standard low-energy equilibrium one [74,75] governing the transport at low temperature [76,77].

Model and GHD solution of domain wall. We consider the unitary dynamics generated by the one-dimensional spin-1/2 XXZ Hamiltonian

$$H = \sum_{x=-\infty}^{\infty} S_x^{\mathrm{x}} S_{x+1}^{\mathrm{x}} + S_x^{\mathrm{y}} S_{x+1}^{\mathrm{y}} + \Delta S_x^{\mathrm{z}} S_{x+1}^{\mathrm{z}}, \tag{1}$$

where S_x^α are spin-1/2 operators acting on the site x. We focus on the regime $-1 < \Delta < 1$ which exhibits ballistic transport [47,78,79]. (It is known that for $|\Delta| > 1$ the domain wall does not melt—see, e.g., the energetic argument given in Refs. [80,81]—and $\Delta = 1$ is pathological [51,82].) Moreover, we focus on the "rational case" where the anisotropy Δ is parameterized as

$$\Delta = \cos(\gamma), \quad \gamma = \pi\, Q/P, \tag{2}$$

where Q and P are two coprime integers with $1 \leqslant Q < P$. The initial state is the classical DW state in the z direction, $|\mathrm{DW}\rangle = |\cdots\uparrow\uparrow\uparrow\downarrow\downarrow\downarrow\cdots\rangle$ and it undergoes unitary evolution generated by the Hamiltonian (1), i.e., $|\Psi(t)\rangle = e^{-itH}|\mathrm{DW}\rangle$. In Ref. [47], the exact large-time magnetization profile was calculated using GHD, as we now briefly recall. GHD is a hydrodynamic approach valid at large distances and on long timescales, where the local state of the system in a space-time cell $[x, x+dx]\times[t, t+dt]$ is represented by a Fermi filling factor $\vartheta_j(x,t,\lambda)\in[0,1]$ for each species j of quasiparticles, or string, with rapidity λ [33]. For the XXZ chain in the rational case, the index j is an integer ranging from 1 to $\ell = \sum_{k=1}^{\delta}\nu_k$, where the ratio Q/P has been represented as a finite continued fraction $Q/P = \frac{1}{\nu_1+\frac{1}{\nu_2+\cdots}}$ of length δ [83]. The GHD equations then read [33,41]

$$\partial_t\vartheta_j(\lambda;x,t) + v_j^{\mathrm{eff}}(\lambda)\partial_x\vartheta_j(\lambda;x,t) = 0, \tag{3a}$$

$$v_j^{\mathrm{eff}}(\lambda) = \frac{\partial_\lambda\varepsilon(\lambda)}{\partial_\lambda p(\lambda)}, \tag{3b}$$

where $\varepsilon_j(\lambda)$ and $p_j(\lambda)$ are the energy and momentum of a quasiparticle of species j with rapidity λ. Their explicit expressions is not essential for us and can be found in Ref. [84]. For general initial states, the GHD equations have to be solved numerically [33,34], but for the special case of the DW initial state they admit an analytical solution [47]. This stems from two remarkable observations: (i) In the initial state, all filling factors are identically zero or one, i.e., $\vartheta_j(\lambda;x,t=0)=1$ for $j\in\{\ell-1,\ell\}$ and $\lambda<0$ and vanishes otherwise; and (ii) in those local macrostates the effective velocity takes a very simple form independent of space and time,

$$v_j^{\mathrm{eff}}(\lambda) = \frac{\sin(\pi Q/P)}{\sin(\pi/P)}\sin(\sigma_j p_j(\lambda)), \quad j\in\{\ell,\ell-1\}, \tag{4}$$

where $\sigma_j = \mathrm{sgn}(p_j'(0))$ is the "sign" of the string, defined so that $\sigma_j p_j(\lambda)$ is a strictly increasing function of $\lambda\in[-\pi/P,\pi/P]$. Then Eq. (3a) is easily solved [47],

$$\vartheta_j(\lambda;x,t) = \begin{cases} 1 & \text{if} \quad x/t > v_j^{\mathrm{eff}}(\lambda) \quad \text{and} \quad j\in\{\ell-1,\ell\} \\ 0 & \text{otherwise.}\end{cases} \tag{5}$$

The local macrostate parameterized by the filling factor $\vartheta_j(x,t,\lambda)$ thus depends only on the ratio $\zeta = x/t$; this is, of course, expected since the problem of domain-wall melting is a particular case of the more general Riemann problem in hydrodynamics [85]. The velocity does not depend explicitly on x/t, but the effect of the interactions is such that the light-cone is shrunk as $x/t\in[-\sin(\gamma),\sin(\gamma)]$. This led to analytic formulas for the profiles of the stationary magnetization and spin current [47] (see also Ref. [84] for a short summary).

Effective LL for quantum fluctuations in the melted region. The goal of this paper is to investigate quantities that go beyond the classical Euler-scale GHD equations [(3a) and (3b)], such as the bipartite entanglement entropy or the quantum fluctuations of the magnetization. This requires us to describe quantum fluctuations around the GHD solution. The dynamics from the DW state is fully characterized by the last two strings. In particular, for any ray $\zeta = x/t$, each of them has one single Fermi point λ^* where the filling factor $\vartheta(\lambda^*;x,t)$ jumps from 0 to 1. Quite generally, in this kind of zero-entropy states, one can expect that quantum fluctuations can be captured by an effective inhomogeneous LL [70,86,87]. The action of this effective field theory is of the form

$$\mathcal{S} = \frac{1}{8\pi}\int\frac{\sqrt{-\det g}\,dxdt}{K}g^{ab}(\partial_a h)(\partial_b h), \tag{6}$$

where $a,b = x,t$ and $h(x,t)$ is the height field related to the fluctuations of the local magnetization as $S_x^z - \langle S_x^z\rangle = \frac{1}{2\pi}\partial_x h$. The effective action (6) contains two free parameters: the metric g with Lorentzian signature [more precisely, $\mathcal{S}$ depends only on the conformal class of the metric g, since the action is invariant under Weyl transformation $g\to\lambda(x,t)g$], and the Luttinger parameter K. Since the system is inhomogeneous, both g and K may depend on the spacetime coordinate (x,t).

We start by fixing the metric in Eq. (6): It must be of the form $ds^2 = (v_\ell dt - dx)(v_{\ell-1}dt - dx)$, where v_ℓ and $v_{\ell-1}$ are the velocities of quasiparticle excitations around the Fermi point λ^* for the quasiparticle species $j=\ell$ and $j=\ell-1$ respectively. Here the quasiparticles are all emitted from the domain wall at $x=0$ at time $t=0$, and therefore in order to arrive at position x at time t they must be traveling at the same velocity $v_\ell = v_{\ell-1} = x/t$. Thus, the metric is $ds^2 = (\frac{x}{t}dt - dx)^2$. This metric is degenerate (see also Ref. [86] for a discussion of the particular case $\Delta=0$); however, in practice one can compute correlation functions assuming $v_\ell\neq v_{\ell-1}$, such that the metric is nondegenerate, and then take $v_\ell\to v_{\ell-1}$ at the end of all calculations.

Then, we fix the Luttinger parameter K in Eq. (6). As in standard Luttinger liquid theory, the excess density of particles or magnetization $\rho(x) = \frac{1}{2\pi}\partial_x h$ is related to the excess density of quasiparticles $\tilde{\rho}$ traveling freely through the system by $\rho(x,t) = \sqrt{K}\tilde{\rho}(x,t)$ [74], so the Luttinger parameter K may be viewed as the square of the quasiparticle charge [88]. K can be extracted from finite-size energy corrections around the ground state (see for instance Eq. (9.18) in Chapter I or Eq. (5.3) in Chapter II of Ref. [89]) but also more generally around zero-entropy states [68] which include our local quasistationary states. When the latter quasistationary state has only two Fermi points, the Luttinger parameter is the square of the dressed magnetization evaluated at any of the two Fermi points [68,89]. A direct calculation of the dressed magnetization in our quasistationary states leads to the following value of K [84], independently of x and t:

$$K = \frac{P^2}{4}. \tag{7}$$

Remarkably, since K depends only on the denominator of γ/π, it exhibits a fractal (i.e., nowhere continuous) dependence on the anisotropy parameter $\Delta = \cos(\gamma)$. Also, since the Luttinger parameter does not depend on x and t, this is a particularly simple version of an inhomogeneous LL where conformal invariance is not broken [87]. Consequently, the correlation functions of primary fields ϕ_1, ..., ϕ_n with scaling dimensions Δ_1, ..., Δ_n obey the scaling relation

$$\langle\phi_1(x_1,t_1)\ldots\phi_n(x_n,t_n)\rangle = \prod_{i=1}^{n}(\tau/t_i)^{\Delta_i}\langle\phi_1(\tau x_1/t_1,\tau)\ldots\phi_n(\tau x_n/t_n,\tau)\rangle \tag{8}$$

for any fixed τ. In other words, all correlation functions can be expressed in terms of equal-time correlations at some fixed time τ. However, we cannot yet fully determine the correlation functions at time τ, as this would require an exact lattice calculation. In the free fermion case $\Delta = 0$, such a calculation is possible [86] using a clever Euclidean-time regularization which connects to a two-dimensional inhomogeneous statistical problem [90]. In principle, a similar regularization should also be possible for $\Delta \neq 0$ [91], but presently we do not know how to do this calculation. Nevertheless, the scaling relation (8) is sufficient to derive a number of nontrivial results about quantum correlations in the long-time behavior of the system which we summarize in the following.

Entanglement entropy. We consider the entanglement entropy for the bipartition $A = (-\infty, x-1]$ and $B = [x, \infty)$, i.e., $S_\alpha(x,t) = \frac{1}{1-\alpha}\ln(\mathrm{Tr}[\rho_A^\alpha(t)])$, where $\rho_A(t) = \mathrm{Tr}_B|\Psi(t)\rangle\langle\Psi(t)|$ is the reduced density matrix of subsystem A. In the effective Luttinger liquid description, the trace $\mathrm{Tr}[\rho_A^\alpha(t)]$ can be obtained as the expectation value of a twist field $\langle\phi(x,t)\rangle$ in a theory with replicas [92]. The twist field ϕ is a primary operator with scaling dimension $\Delta = \frac{1}{12}(\alpha - 1/\alpha)$; therefore, the scaling relation (8) leads to

$$\begin{aligned} S_\alpha(x,t) &= \frac{1}{1-\alpha}\ln(\langle\phi(x,t)\rangle/\epsilon) \\ &= \frac{1}{1-\alpha}\ln((\tau/t)^{\frac{1}{24}(\alpha-\frac{1}{\alpha})}\langle\phi(\tau x/t,\tau)\rangle/\epsilon) \\ &= \frac{1}{12}\left(1+\frac{1}{\alpha}\right)\ln(t/\tau) + f_\alpha(x/t), \end{aligned} \tag{9}$$

where ϵ is a UV length scale which appears when one takes the continuum limit of the lattice model. While for homogeneous systems ϵ is simply a constant, in inhomogeneous setups it depends on the LQSS; in particular, in our setup it can depend on the ratio $\zeta = x/t$. We thus set $f_\alpha(\zeta) = \frac{1}{1-\alpha}\ln[\langle\phi(\tau\zeta,\tau)\rangle/\epsilon(\zeta)]$, which is an unknown function of ζ.

When evaluated at fixed x and in the limit $t \to \infty$, the entanglement entropy therefore exhibits a leading logarithmic universal behavior. For the von Neumann entropy ($\alpha \to 1$), this gives

$$S_1(x,t) \underset{\substack{t\to\infty \\ x \text{ fixed}}}{\sim} \frac{1}{6}\ln t + c_0(\Delta) + o(1), \tag{10}$$

where the subleading term $c_0(\Delta)$ eventually depend on Δ. In the top left panel of Fig. 1, we show the entanglement entropy $S_1(x=0,t)$. The perfect logarithmic behavior, with a prefactor independent of the value of the anisotropy Δ and compatible with the predicted value 1/6, nicely confirms the expectations from the LL description of the melted region. The equilibration occurs much more quickly for smaller values of the denominator P; for $Q/P = 1/2$ and 1/3, the large-time stationary regime has been reached at accessible times and the entanglement entropy perfectly matches the logarithmic growth (10). Also for $Q/P = 1/4$, the approach to the LL regime is evident, despite the presence of slowly decaying oscillations. Remarkably, for $Q/P = 2/5$, although the value of the anisotropy is relatively small, $\Delta \simeq 0.309$, the relaxation toward the asymptotic regime is very slow. Notice finally that for $Q/P = 1/5$ and 2/5, the entanglement entropy approaches the LL asymptotics oscillating around the same curve, implying that the nonuniversal additive constant $c_0(\Delta)$ is the same for the two cases. This observation suggests that $c_0(\Delta)$ may depend only on P (i.e., K), although we do not have a field-theory explanation supporting this. Finally, to shed further light on the entanglement dynamics, we show the case $\Delta = \cos(\pi 49/100) \simeq 0.031$ in Fig. 1. It completely differs from the noninteracting case: The entanglement entropy grows much more quickly, confirming that it has not yet reached the asymptotic logarithmic behavior.

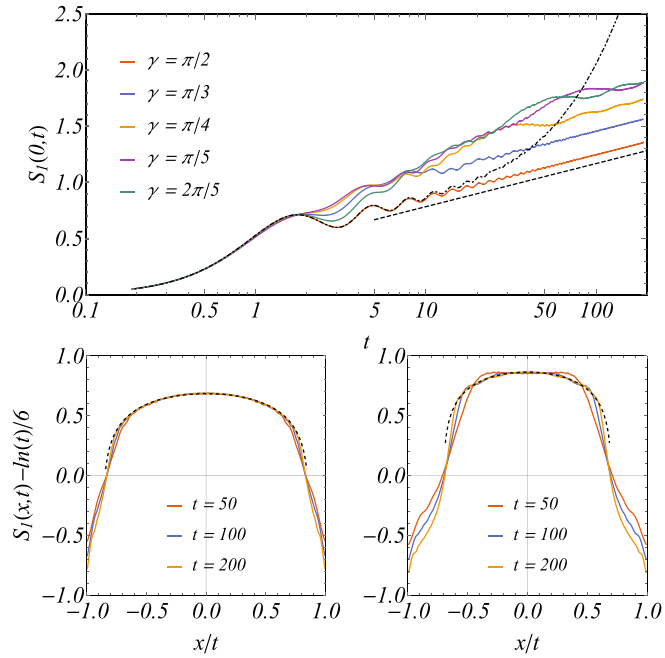

FIG. 1. (Top panel) The time evolution of the entanglement entropy between the two halves of the system, namely $[-L/2,-1]$ and $[0, L/2-1]$, is plotted in log-linear scale. Different colors represent the Time Evolving Block Decimation (TEBD) simulations for different values of the anisotropy Δ. The black dashed line is a guide for the eyes, representing the asymptotic leading behavior $\sim \ln(t)/6$. The black dot-dashed line shows the behavior for $\gamma/\pi = 49/100 = 0.49$, which completely differs from the noninteracting case ($\gamma/\pi = 1/2$). (Bottom panels) The profiles of the entanglement entropy as a function of the ray x/t for different times t and $\gamma = \pi/3$ (left), $\pi/4$ (right). The black dashed lines are the phenomenological approximation (11).

Next, we study the entanglement entropy $S_1(x,t)$ for fixed $\zeta = x/t$ when $t \to \infty$. As explained above, the profile function $f_1(\zeta)$ is hard to compute because it gets contributions both from the field theory and from the lattice regularization. Nevertheless, we can calculate it numerically, as shown in Fig. 1. The numerical results are well approximated by the phenomenological formula

$$f_1(\zeta) \simeq \frac{1}{6}\left(1+\frac{1}{P}\right)\ln\left[1-\left(\frac{\zeta}{\sin(\gamma)}\right)^2\right], \tag{11}$$

designed such that for $Q/P = 1/2$ it reproduces the exact result for $\Delta = 0$ [86]. We do not have a theoretical justification of Eq. (11), but nonetheless it undeniably provides a rather good approximation.

In Fig. 1 (left bottom panel), we show the profile of the entanglement entropy for $Q/P = 1/3$ and different times [larger than 50 for which system is in the LQSS from the measure of $S_1(0,t)$]. The profile is well approximated by Eq. (11), excepts from tiny regions close to the light cone $x/t \simeq \pm\sin(\gamma)$. For $Q/P = 1/4$ (right bottom panel in Fig. 1), the largest time accessible by time-evolving block decimation (TEBD) [93] simulations is not sufficient to observe a complete relaxation to the large-time stationary behavior. For this reason, oscillations on top of the asymptotic profile are present, but the agreement with Eq. (11) is fairly good.

Full counting statistics. We now turn to the fluctuations of the magnetization $M_{[x_1,x_2]} = \sum_{x=x_1}^{x_2} S_x^z$ in an interval $[x_1, x_2]$ inside the melted region. The generating function of the cumulants is

$$F_{[x_1,x_2]}(\lambda,t) = \left\langle \exp\left(-i\lambda M_{[x_1,x_2]}\right)\right\rangle_t = \left\langle e^{i\frac{\lambda}{2\pi}h(x_1,t)} e^{-i\frac{\lambda}{2\pi}h(x_2,t)}\right\rangle, \tag{12}$$

where in the second line we used that the local magnetization is related to the height field as $S_x^z - \langle S_x^z\rangle = \frac{1}{2\pi}\partial_x h$. We are interested in the case of an interval $[x - l/2, x + l/2]$ with fixed length $l \gg 1$, in limit of large time $t \gg l$, keeping $\zeta = x/t$ fixed. In that limit, the point $x - l/2$ and $x + l/2$ look very close to each other, so we may use the operator product expansion of the primary field $e^{\pm i\alpha h(x,t)}$ to evaluate the scaling behavior of the generating function: $e^{-i\alpha h(x+l/2,t)} e^{i\alpha h(x-l/2,t)} \sim l^{-2\Delta} + \cdots$, where $\Delta = \alpha^2 K$ is the scaling dimension of the primary field. Thus, at large times the generating function behaves as

$$F_{[x-l/2,x+l/2]}(\lambda,t) \simeq \left(\frac{l}{\epsilon'(x/t)}\right)^{-\frac{\lambda^2}{2\pi^2}K}, \tag{13}$$

where ϵ' is a UV length scale, similar to but different from ϵ, which may also depend on ζ.

The numerical study of the full counting statistics in the LQSS is tricky due to its dependence on the subsystem size l. Indeed, Eq. (13) works only if the actual time reached by the unitary evolution is sufficiently large to guarantee a complete generalized thermalization of the entire subsystem $[x - l/2, x + l/2]$. The dependence on ϵ' is canceled by considering the logarithm of the ratio between two different subsystem sizes, specifically,

$$\mathcal{F}(\lambda) \equiv \log_2\left[\frac{F_{[x-l,x+l]}(\lambda,t)}{F_{[x-l/2,x+l/2]}(\lambda,t)}\right] \underset{t\gg l\gg 1}{\simeq} -\frac{K}{2\pi^2}\lambda^2. \tag{14}$$

Since both subsystems should be almost stationary, we focus on relatively small intervals, namely $l = 4$, 8, and 16. In Fig. 2, we plot $\mathcal{F}(\lambda)$ for the subsystem at $x = 0$ for $Q/P = 1/2$, $1/3$, $1/4$, and $1/5$ at the maximum accessible time $t \simeq 200$. Notice that the approach to the asymptotic behavior is not monotonic in l (since the information spreads out from the junction, the subsystem of size $2l$ takes longer to reach stationarity). Interestingly, all curves approach the stationary behavior from the neighborhood of $\lambda = 0$. For this reason, it is more instructive to analyze the variance of the subsystem magnetization, i.e., the second cumulant, as a function of the subsystem size, both in the center of the system at $\zeta = 0$ and away from it.

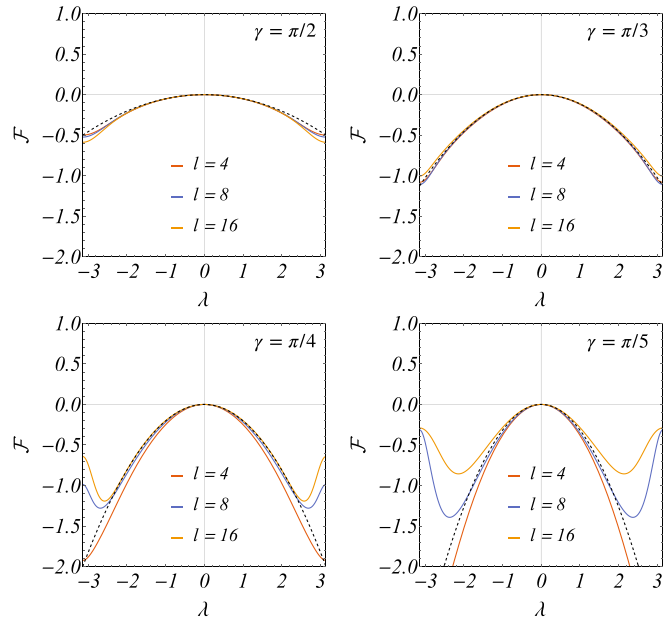

FIG. 2. The logarithm of the ratio of generating functions at the largest time $t \simeq 200$ for different subsystem sizes l and parameter γ. The black dashed lines represent the LL quadratic prediction (14).

Fluctuations of subsystem magnetization. The variance of the magnetization in the interval $[x - l/2, x + l/2]$ follows from Eq. (13) as

$$\left\langle M^2_{[x-l/2,x+l/2]}\right\rangle_t - \langle M_{[x-l/2,x+l/2]}\rangle_t^2 = -\frac{1}{2}\partial_\lambda^2 \log F_{[x-l/2,x+l/2]}|_{\lambda=0} \underset{t\gg l\gg 1}{\simeq} \frac{K}{\pi^2}\log(l) + O(1). \tag{15}$$

In Fig. 3, we show the results obtained at $\zeta = x/t = 0$ and $\zeta \simeq 1/4$ for $l \in [2, 50]$ and at $t \simeq 200$. For nonzero ζ, the numerical analysis is slightly more difficult: The convergence is unavoidably poorer than at $\zeta = 0$ because the approach to the LQSS requires more time as we move away from the junction. Some comments are due: (1) The numerical

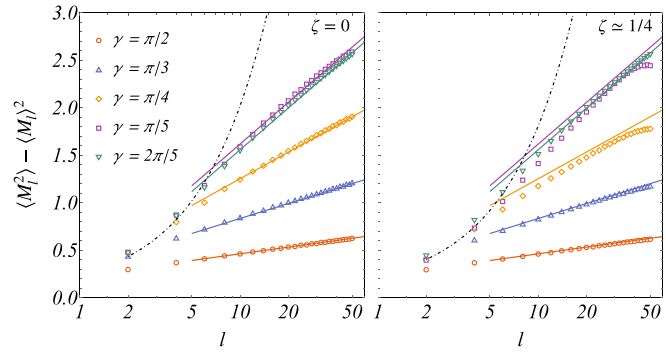

FIG. 3. The TEBD data for the variance of the subsystem magnetization (symbols) at the largest accessible time $t \simeq 200$ are compared with the LL predictions (full lines). The subsystems are centered around $\zeta = 0$ (left) and $\zeta \simeq 1/4$ (right). For comparison, the black dot-dashed line is the $\gamma/\pi = 49/100$ case, which is not yet stationary.

data for all ζ manifest an asymptotic tendency toward the right logarithmic behavior also with the same nonuniversal constant; the full lines are indeed the same in both panels. (2) For $\zeta \simeq 1/4$, the data show larger finite-size/finite-time effects because the subsystem is closer to the propagating front (the center of the subsystem is located at $x = 50$ for $t = 200$); hence, the subsystem is not relaxed for large l when the numerical data deviate from the scaling prediction. (3) Very remarkably, the numerical simulations, both for $\zeta = 0$ and $\zeta \simeq 1/4$, show the same asymptotic behavior for two very different values of the anisotropy, namely $\Delta = \cos(\pi/5) \simeq 0.809$ and $\Delta = \cos(2\pi/5) \simeq 0.309$, confirming that the only parameter entering in the large-scale/large-time description of the local quasistationary state is the square of the quasiparticle charge (7), which depends only on P, the denominator of γ/π; see Eq. (2). Again, in order to further support this scenario, we also show data for $\Delta = \cos(\pi 49/100) \simeq 0.031$, which are far from equilibrated and very different from the $\gamma/\pi = 1/2$ case.

Discussions and conclusions. In this Rapid Communication, we analytically showed that the stationary state resulting from the melting of a domain wall in an XXZ chain is described at low energy (i.e., large times and distances) by an emergent Luttinger liquid with Luttinger parameter nowhere continuous in Δ. We corroborate this surprising prediction by accurate numerical tensor network simulations which strongly support our finding, manifested in the central charge of the underlying field theory being 1 (from the measure of the entanglement entropy) and in the Luttinger parameter being $K = P^2/4$ (from measures of the magnetization statistics). We stress that it is a nontrivial consequence of the emergent conformal invariance that we demonstrate here, that two-time correlation functions can be related from equal-time ones. As a consequence, the fractal behavior already observed in genuinely dynamical quantities (e.g., the spin Drude weight [79,94–97]) appears also in the Luttinger parameter and consequently in equal-time correlators.

In spite of these robust and intriguing findings, there are still many open questions. First, it would be interesting to determine correlation functions in the LQSS to provide further predictions to be tested numerically also to have further confirmations of the fractal Luttinger scenario; unfortunately, this is still beyond our technical capabilities. Another important question concerns the generality of our scenario: Are there in more complicated integrable models (such as higher spin chains or Hubbard models, studied already with GHD [98–100]) zero entropy initial states with an LQSS being a fractal Luttinger liquid? What is the nature of the LQSS at the isotropic point $\Delta = 1$ with pathological transport [81]?

Finally, we note that the domain-wall problem resembles the spatiotemporal quench protocol [101] for fast preparation of quantum critical systems. The idea is that, contrary to low-energy states of gapless systems—which cannot be reached easily by cooling because temperatures would have to be prohibitively low—product states can be engineered easily in cold atom experiments [102] and then be evolved unitarily. Thus, the domain-wall melting problem can be viewed as a realistic protocol for fast preparation of a Luttinger liquid, similarly to the protocol of Ref. [101]. Our results show that the critical system engineered in this way will indeed be a Luttinger liquid, but it will be very different from the one corresponding to the ground state of the XXZ chain.

Acknowledgements. We thank J. Viti for useful discussions and collaboration on related topics. P.C. acknowledges support from ERC under Consolidator Grant No. 771536 (NEMO).

[1] J. Torrance and M. Tinkham, Excitation of multiple-magnon bound states in $CoCl_2 \cdot 2H_2O$, Phys. Rev. **187**, 595 (1969).
[2] I. G. Gochev, Spin complexes in a bounded chain, JETP **26**, 3 (1977).
[3] I. G. Gochev, Contribution to the theory of plane domain walls in a ferromagnet, JETP **58**, 115 (1983).
[4] S. Yuan, H. De Raedt, and S. Miyashita, Domain-wall dynamics near a quantum critical point, Phys. Rev. B **75**, 184305 (2007).
[5] O. Gamayun, Y. Miao, and E. Ilievski, Domain-wall dynamics in the Landau-Lifshitz magnet and the classical-quantum correspondence for spin transport, Phys. Rev. B **99**, 140301(R) (2019).
[6] T. Antal, Z. Rácz, A. Rákos, and G. Schütz, Transport in the XX chain at zero temperature: Emergence of flat magnetization profiles, Phys. Rev. E **59**, 4912 (1999).
[7] V. Hunyadi, Z. Rácz, and L. Sasvári, Dynamic scaling of fronts in the quantum XX chain, Phys. Rev. E **69**, 066103 (2004).
[8] T. Platini and D. Karevski, Scaling and front dynamics in Ising quantum chains, Eur. Phys. J. B **48**, 225 (2005).
[9] T. Platini and D. Karevski, Relaxation in the XX quantum chain, J. Phys. A **40**, 1711 (2007).
[10] A. De Luca, J. Viti, D. Bernard, and B. Doyon, Nonequilibrium thermal transport in the quantum Ising chain, Phys. Rev. B **88**, 134301 (2013).
[11] A. De Luca, G. Martelloni, and J. Viti, Stationary states in a free fermionic chain from the quench action method, Phys. Rev. A **91**, 021603 (2015).
[12] J. Viti, J.-M. Stéphan, J. Dubail, and M. Haque, Inhomogeneous quenches in a free fermionic chain: Exact results, EPL **115**, 40011 (2016).
[13] V. Eisler, F. Maislinger, and H. G. Evertz, Universal front propagation in the quantum Ising chain with domain-wall initial states, SciPost Phys. **1**, 014 (2016).
[14] V. Eisler and F. Maislinger, Hydrodynamical phase transition for domain-wall melting in the XY chain, Phys. Rev. B **98**, 161117(R) (2018).
[15] M. Kormos, Inhomogeneous quenches in the transverse field Ising chain: Scaling and front dynamics, SciPost Phys. **3**, 020 (2017).
[16] S. Bhattacharyya and S. Dasgupta, Dynamics in quantum Ising chain driven by inhomogeneous transverse magnetization, Eur. Phys. J. B **90**, 140 (2017).
[17] D. Gobert, C. Kollath, U. Schollwöck, and G. M. Schütz, Real-time dynamics in spin-1/2 chains with adaptive

time-dependent density matrix renormalization group, Phys. Rev. E **71**, 036102 (2005).
[18] S. Jesenko and M. Znidaric, Finite-temperature magnetization transport of the one-dimensional anisotropic Heisenberg model, Phys. Rev. B **84**, 174438 (2011).
[19] P. Calabrese, C. Hagendorf, and P. Le Doussal, Time evolution of 1D gapless models from a domain-wall initial state: SLE continued?, J. Stat. Mech. (2008) P07013.
[20] V. Zauner, M. Ganahl, H. Evertz, and T. Nishino, Time evolution within a comoving window: Scaling of signal fronts and magnetization plateaus after a local quench in quantum spin chains, J. Phys.: Condens. Matter **27**, 425602 (2012).
[21] J. Halimeh, A. Wöllert, I. McCulloch, U. Schollwöck, and T. Barthel, Domain-wall melting in ultracold-boson systems with hole and spin-flip defects, Phys. Rev. A **89**, 063603 (2014).
[22] V. Alba and F. Heidrich-Meisner, Entanglement spreading after a geometric quench in quantum spin chains, Phys. Rev. B **90**, 075144 (2014).
[23] J. Hauschild, F. Heidrich-Meisner, and F. Pollmann, Domain-wall melting as a probe of many-body localization, Phys. Rev. B **94**, 161109(R) (2016).
[24] T. Sabetta and G. Misguich, Nonequilibrium steady states in the quantum XXZ spin chain, Phys. Rev. B **88**, 245114 (2013).
[25] C. Karrasch, R. Ilan, and J. E. Moore, Nonequilibrium thermal transport and its relation to linear response, Phys. Rev. B **88**, 195129 (2013).
[26] A. Biella, A. De Luca, J. Viti, D. Rossini, L. Mazza, and R. Fazio, Energy transport between two integrable spin chains, Phys. Rev. B **93**, 205121 (2016).
[27] A. De Luca, J. Viti, L. Mazza, and D. Rossini, Energy transport in Heisenberg chains beyond the Luttinger liquid paradigm, Phys. Rev. B **90**, 161101(R) (2014).
[28] D. Bernard and B. Doyon, Conformal field theory out of equilibrium: A review, J. Stat. Mech. (2016) 064005.
[29] B. Doyon, A. Lucas, K. Schalm, and M. J. Bhaseen, Non-equilibrium steady states in the Klein-Gordon theory, J. Phys. A **48**, 095002 (2015).
[30] L. Vidmar, D. Iyer, and M. Rigol, Emergent Eigenstate Solution to Quantum Dynamics Far from Equilibrium, Phys. Rev. X **7**, 021012 (2017).
[31] T. Rakovszky, C. von Keyserlingk, and F. Pollmann, Entanglement growth after inhomogenous quenches, Phys. Rev. B **100**, 125139 (2019).
[32] V. Bulchandani and C. Karrasch, Subdiffusive front scaling in interacting integrable models, Phys. Rev. B **99**, 121410(R) (2019).
[33] B. Bertini, M. Collura, J. De Nardis, and M. Fagotti, Transport in Out-of-Equilibrium XXZ Chains: Exact Profiles of Charges and Currents, Phys. Rev. Lett. **117**, 207201 (2016).
[34] O. Castro-Alvaredo, B. Doyon, and T. Yoshimura, Emergent Hydrodynamics in Integrable Quantum Systems Out of Equilibrium, Phys. Rev. X **6**, 041065 (2016).
[35] B. Doyon, and T. Yoshimura, A note on generalized hydrodynamics: Inhomogeneous fields and other concepts, SciPost Phys. **2**, 014 (2017).
[36] B. Doyon, J. Dubail, R. Konik, and T. Yoshimura, Large-Scale Description of Interacting One-Dimensional Bose Gases: Generalized Hydrodynamics Supersedes Conventional Hydrodynamics, Phys. Rev. Lett. **119**, 195301 (2017).
[37] V. Bulchandani, R. Vasseur, C. Karrasch, and J. Moore, Bethe-Boltzmann hydrodynamics and spin transport in the XXZ chain, Phys. Rev. B **97**, 045407 (2018).
[38] M. Gruber and V. Eisler, Magnetization and entanglement after a geometric quench in the XXZ chain, Phys. Rev. B **99**, 174403 (2019).
[39] A. Bastianello, V. Alba, and J.-S. Caux, Generalized Hydrodynamics with Space-Time Inhomogeneous Interactions, Phys. Rev. Lett. **123**, 130602 (2019).
[40] D.-L. Vu and T. Yoshimura, Equations of state in generalized hydrodynamics, SciPost Phys. **6**, 023 (2019).
[41] M. Borsi, B. Pozsgay, and L. Pristyák, Current Operators in Bethe Ansatz and Generalized Hydrodynamics: An Exact Quantum/Classical Correspondence, Phys. Rev. X **10**, 011054 (2020).
[42] B. Pozsgay, Current operators in integrable spin chains: Lessons from long range deformations, SciPost Phys. **8**, 016 (2020).
[43] F. S. Moller and J. Schmiedmayer, Introducing iFluid: A numerical framework for solving hydrodynamical equations in integrable models, SciPost Phys. **8**, 041 (2020).
[44] A. Bastianello, B. Doyon, G. Watts, and T. Yoshimura, Generalized hydrodynamics of classical integrable field theory: The sinh-Gordon model, SciPost Phys. **4**, 045 (2018).
[45] B. Doyon and H. Spohn, Dynamics of hard rods with initial domain wall state, J. Stat. Mech. (2017) 073210.
[46] B. Doyon, H. Spohn, and T. Yoshimura, A geometric viewpoint on generalized hydrodynamics, Nucl. Phys. B **926**, 570 (2017)
[47] M. Collura, A. De Luca, and J. Viti, Analytic solution of the domain-wall nonequilibrium stationary state, Phys. Rev. B **97**, 081111(R) (2018).
[48] J. De Nardis, D. Bernard, and B. Doyon, Hydrodynamic Diffusion in Integrable Systems, Phys. Rev. Lett. **121**, 160603 (2018).
[49] S. Gopalakrishnan, D. A. Huse, V. Khemani, and R. Vasseur, Hydrodynamics of operator spreading and quasiparticle diffusion in interacting integrable systems, Phys. Rev. B **98**, 220303(R) (2018).
[50] M. Panfil and J. Pawełczyk, Linearized regime of the generalized hydrodynamics with diffusion, SciPost Phys. Core **1**, 002 (2019).
[51] E. Ilievski, J. De Nardis, M. Medenjak, and T. Prosen, Superdiffusion in One-Dimensional Quantum Lattice Models, Phys. Rev. Lett. **121**, 230602 (2018).
[52] B. Doyon, Diffusion and superdiffusion from hydrodynamic projection, arXiv:1912.01551.
[53] L. Piroli, J. De Nardis, M. Collura, B. Bertini, and M. Fagotti, Transport in out-of-equilibrium XXZ chains: Nonballistic behavior and correlation functions, Phys. Rev. B **96**, 115124 (2017).
[54] A. Biella, M. Collura, D. Rossini, A. De Luca, and L. Mazza, Ballistic transport and boundary resistances in inhomogeneous quantum spin chains, Nat. Commun. **10**, 4820 (2019).
[55] A. J. Friedman, S. Gopalakrishnan, and R. Vasseur, Diffusive hydrodynamics from integrability breaking, Phys. Rev. B **101**, 180302 (2020).
[56] A. Bastianello and A. De Luca, Integrability-Protected Adiabatic Reversibility in Quantum Spin Chains, Phys. Rev. Lett. **122**, 240606 (2019).

[57] J. De Nardis and M. Panfil, Edge Singularities and Quasilong-Range Order in Nonequilibrium Steady States, Phys. Rev. Lett. **120**, 217206 (2018).

[58] M. Fagotti, Higher-order generalized hydrodynamics in one dimension: The noninteracting test, Phys. Rev. B **96**, 220302 (2017).

[59] M. Fagotti, Locally quasi-stationary states in noninteracting spin chains, SciPost Phys. **8**, 048 (2020).

[60] A. Cortés Cubero, How generalized hydrodynamics time evolution arises from a form factor expansion, arXiv:2001.03065.

[61] Y. Brun and J. Dubail, The inhomogeneous Gaussian free field, with application to ground state correlations of trapped 1d Bose gases, SciPost Phys. **4**, 037 (2018).

[62] P. Ruggiero, Y. Brun, and J. Dubail, Conformal field theory on top of a breathing one-dimensional gas of hard core bosons, SciPost Phys. **6**, 051 (2019).

[63] B. Bertini, M. Fagotti, L. Piroli, and P. Calabrese, Entanglement evolution and generalised hydrodynamics: noninteracting systems, J. Phys. A **51**, 39LT01 (2018).

[64] V. Alba, Towards a generalized hydrodynamics description of Rényi entropies in integrable systems, Phys. Rev. B **99**, 045150 (2019).

[65] V. Alba, B. Bertini, and M. Fagotti, Entanglement evolution and generalised hydrodynamics: Interacting integrable systems, SciPost Phys. **7**, 005 (2019).

[66] A. Bastianello, J. Dubail, and J.-M. Stéphan, Entanglement entropies of inhomogeneous Luttinger liquids, J. Phys. A: Math. Theor. **53**, 155001 (2020).

[67] T. Fokkema, S. Eliëns, and J.-S. Caux, Split Fermi seas in one-dimensional Bose fluids, Phys. Rev. A **89**, 033637 (2014).

[68] S. Eliëns and J.-S. Caux, General finite-size effects for zero-entropy states in one-dimensional quantum integrable models, J. Phys. A **49**, 495203 (2016).

[69] R. Vlijm, S. Eliëns, and J.-S. Caux, Correlations of zero-entropy critical states in the XXZ model: Integrability and Luttinger theory far from the ground state, SciPost Phys. **1**, 008 (2016).

[70] P. Ruggiero, P. Calabrese, B. Doyon, and J. Dubail, Quantum Generalized Hydrodynamics, Phys. Rev. Lett. **124**, 140603 (2020).

[71] B. Bertini and M. Fagotti, Determination of the Nonequilibrium Steady State Emerging from a Defect, Phys. Rev. Lett. **117**, 130402 (2016).

[72] A. Bastianello and A. De Luca, Nonequilibrium Steady State Generated by a Moving Defect: The Supersonic Threshold, Phys. Rev. Lett. **120**, 060602 (2018).

[73] A. Bastianello and A. De Luca, Superluminal moving defects in the Ising spin chain, Phys. Rev. B **98**, 064304 (2018).

[74] T. Giamarchi, *Quantum Physics in One Dimension* (Clarendon Press, Oxford, 2003).

[75] J. Sirker and M. Bortz, The open XXZ-chain: Bosonisation, Bethe ansatz, and logarithmic corrections, J. Stat. Mech. (2006) P01007.

[76] B. Bertini, L. Piroli, and P. Calabrese, Universal Broadening of the Light Cone in Low-Temperature Transport, Phys. Rev. Lett. **120**, 176801 (2018).

[77] B. Bertini and L. Piroli, Low-temperature transport in out-of-equilibrium XXZ chains, J. Stat. Mech. (2018) 033104.

[78] T. Prosen and E. Ilievski, Families of Quasilocal Conservation Laws and Quantum Spin Transport, Phys. Rev. Lett. **111**, 057203 (2013).

[79] E. Ilievski and J. De Nardis, Microscopic Origin of Ideal Conductivity in Integrable Quantum Models, Phys. Rev. Lett. **119**, 020602 (2017).

[80] G. Misguich, K. Mallick, and P. L. Krapivsky, Dynamics of the spin-1/2 Heisenberg chain initialized in a domain-wall state, Phys. Rev. B **96**, 195151 (2017).

[81] G. Misguich, N. Pavloff, and V. Pasquier, Domain wall problem in the quantum XXZ chain and semiclassical behavior close to the isotropic point, SciPost Phys. **7**, 025 (2019).

[82] M. Ljubotina, M. Znidaric, and T. Prosen, Spin diffusion from an inhomogeneous quench in an integrable system, Nat. Commun. **8**, 16117 (2017).

[83] M. Takahashi, *Thermodynamics of One-Dimensional Solvable Models* (Cambridge University Press, Cambridge, UK, 1999).

[84] See Supplemental Material at http://link.aps.org/supplemental/10.1103/PhysRevB.102.180409 for details about numerical implementation, a summary of the GHD solution of the DW state, and the calculation of the Luttinger parameter from the dressed magnetizations; it also includes Refs. [47,83,93].

[85] B. Riemann, Über die Fortpflanzung ebener Luftwellen von endlicher Schwingungsweite, Abhandlungen der Geselschaft der Wissenschaften zu Göttingen, Mathematisch-Physicalische Klasse **8**, 43 (1860).

[86] J. Dubail, J.-M. Stéphan, J. Viti, and P. Calabrese, Conformal field theory for inhomogeneous one-dimensional quantum systems: The example of non-interacting Fermi gases, SciPost Phys. **2**, 002 (2017).

[87] J. Dubail, J.-M. Stéphan and P. Calabrese, Emergence of curved light-cones in a class of inhomogeneous Luttinger liquids, SciPost Phys. **3**, 019 (2017).

[88] K. Le Hur, B. Halperin, and A. Yacoby, Charge fractionalization in nonchiral Luttinger systems, Ann. Phys. **323**, 3037 (2008).

[89] V. Korepin, N. Bogoliubov, and A. Izergin, *Quantum Inverse Scattering Method and Correlation Functions* (Cambridge University Press, Cambridge, UK, 1997).

[90] N. Allegra, J. Dubail, J.-M. Stéphan, and J. Viti, Inhomogeneous field theory inside the arctic circle, J. Stat. Mech. (2016) 053108.

[91] E. Granet, L. Budzynski, J. Dubail, and J. Jacobsen, Inhomogeneous Gaussian free field inside the interacting arctic curve, J. Stat. Mech. (2019) 013102.

[92] P. Calabrese and J. Cardy, Entanglement entropy and conformal field theory, J. Phys. A **42**, 504005 (2009).

[93] G. Vidal, Efficient Simulation of One-Dimensional Quantum Many-Body Systems, Phys. Rev. Lett. **93**, 040502 (2004).

[94] X. Zotos, Finite Temperature Drude Weight of the One-Dimensional Spin-1/2 Heisenberg Model, Phys. Rev. Lett. **82**, 1764 (1999).

[95] J. Sirker, R. G. Pereira, and I. Affleck, Diffusion and Ballistic Transport in One-Dimensional Quantum Systems, Phys. Rev. Lett. **103**, 216602 (2009).

[96] T. Prosen, Open XXZ Spin Chain: Nonequilibrium Steady State and a Strict Bound on

Ballistic Transport, Phys. Rev. Lett. **106**, 217206 (2011).

[97] A. Urichuk, Y. Oez, A. Klumper, and J. Sirker, The spin Drude weight of the XXZ chain and generalized hydrodynamics, SciPost Phys. **6**, 005 (2019).

[98] E. Ilievski and J. De Nardis, Ballistic transport in the one-dimensional Hubbard model: The hydrodynamic approach, Phys. Rev. B **96**, 081118(R) (2017).

[99] M. Mestyan, B. Bertini, L. Piroli, and P. Calabrese, Spin-charge separation effects in the low-temperature transport of 1D Fermi gases, Phys. Rev. B **99**, 014305 (2019).

[100] Y. Nozawa and H. Tsunetsugu, Generalized hydrodynamic approach to charge and energy currents in the one-dimensional Hubbard model, Phys. Rev. B **101**, 035121 (2020).

[101] K. Agarwal, R. Bhatt, and S. Sondhi, Fast Preparation of Critical Ground States Using Superluminal Fronts, Phys. Rev. Lett. **120**, 210604 (2018).

[102] H. Bernien, S. Schwartz, A. Keesling, H. Levine, A. Omran, H. Pichler, S. Choi, A. Zibrov, M. Endres, M. Greiner, V. Vuletic, and M. Lukin, Probing many-body dynamics on a 51-atom quantum simulator, Nature (London) **551**, 579 (2017).